

# A New Simplified Calculation Model for Torsion Process of Overhead Single Conductors with Light Icing

Ran Li<sup>1</sup>, Zhijin Zhang<sup>1</sup>, Xingliang Jiang<sup>1</sup>, Jianlin Hu<sup>1</sup>, Qin Hu<sup>1</sup>, Hualong Zheng<sup>1</sup>

<sup>1</sup> State Key Laboratory of Power Transmission Equipment & System Security and New Technology, Chongqing University, Shapingba District, Chongqing 400044, China

[20181102022t@cqu.edu.cn](mailto:20181102022t@cqu.edu.cn), [zhangzhijing@cqu.edu.cn](mailto:zhangzhijing@cqu.edu.cn), [xljiang@cqu.edu.cn](mailto:xljiang@cqu.edu.cn), [hujianlin@cqu.edu.cn](mailto:hujianlin@cqu.edu.cn), [huqin@cqu.edu.cn](mailto:huqin@cqu.edu.cn), [hualong.z@foxmail.com](mailto:hualong.z@foxmail.com)

**Abstract**— In this paper, a new simplified calculation model for the torsion process of single conductors with eccentric icing was proposed. The model comprehensively considers the ice thickness difference on the windward and leeward sides of the conductor and the distribution characteristics and time domain update characteristics of the torsional stiffness within the span in the torsion process caused by eccentric icing. Then the model was applied to a 110kV transmission line project in Chongqing, China, and the angles of twist of conductor under 3 groups of pay-off tensions and 3 groups of ice thicknesses were calculated and analyzed. The results showed that under light icing conditions, appropriately increasing the pay-off tensions within the allowable range of the project can inhibit the torsion process, and the suppression effect increases with the increase of the icing thickness. In addition, an icing test in natural environments was carried out at the field test station to verify the proposed simplified torsion model, and the results showed that the average errors of simulated tensions and angles of twist compared with those obtained from experimental measurements were less than 5%.

**Keywords**— *Single conductors, Eccentric icing, Torsional stiffness, Angles of twist, Pay-off tensions*

## I. INTRODUCTION

During the icing process of overhead single conductors, the eccentric icing on the windward side will cause torsion and eventually accumulates into cylindrical or elliptical deposits (shown in Fig. 1) [1-3].

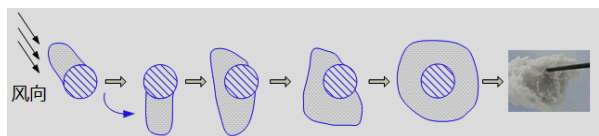


Fig.1 Torsion formation process of cylindrical ice in the natural environment

As a result, on the one hand, the tension level of the conductor is increased, which leads to a decrease in the mechanical safety margin of the transmission line structure; at the same time, the increase of the sag within the span will reduce the electrical insulation safety distance, which is easy to cause flashover and tripping of transmission lines and other issues.

On the other hand, the natural vibration frequency of the conductor will change with the mass distribution characteristics affected by the eccentric icing; under the excitation of specific environmental factors, it is easy to cause vibration damage such as galloping and ice-shedding jump,

etc.; and in serious cases, it can even lead to the collapse of towers, lines breaking and power line outage, causing huge social and economic losses [4-5].

At present, the mainstream research methods on the torsion phenomenon of ice-coated conductors are simulation and field tests.

In [6], the cable torsion caused by ice accretion was modeled and simulated. During the simulation, both ice loads and wind-on-ice loads were taken into account, and the quantity for the wind-on-ice loads was obtained by integrating air pressure and air shear along the airflow boundary. The model was applied to Bersimis cable and an overhead ground wire, and the validity and reliability of the simulation method are verified by comparing with the experimental results. And it is concluded that the torsional stiffness of single conductors can be approximately considered to remain unchanged during the icing process.

[7] analyzed the field test results of a full-scale quad bundle line carried out by KANSAI EPCO, and established the basic parameters for obtaining the torsional stiffness of bundle conductors combined with the corresponding finite element simulation method.

A torsion testing machine was used in [8] to test the torsional stiffness of single conductors with different ice thicknesses. The differences in torsional stiffness of ice-coated conductors with and without creep effect were compared, and the corresponding torsional stiffness fitting formulas for specific conductor types were proposed.

It can be seen from the above that the torsion process of the ice-coated conductor is closely related to its torsional stiffness. In practical engineering, the existing measures with good torsion suppression effects, counterweights (such as detuning pendulums) and spacers (such as interphase spacers and interphase dampers) are based on the principle of increasing the torsional stiffness of conductors [9]. However, once the time-space distribution characteristics of the torsional stiffness of the conductor are taken into account, the corresponding simulation calculation model will become extremely complex, and it is difficult to meet the needs of short time-consuming and efficient solutions in engineering.

Accordingly, this paper proposed a simplified calculation model for the torsion process of ice-coated single conductors that is easy to be solved in engineering. The model comprehensively considered the ice thickness difference between the windward and leeward sides and the distribution

characteristics of torsional stiffness within the span, and reasonably updated the ice weight and torsional moment based on the principle of small deformation. Based on the structural parameters of a 110 kV transmission line project in Chongqing, China, the shape-finding analysis of single conductors under 3 groups of different tensions and the calculation of angles of twist and torsional stiffness under different degrees of icing were carried out, and the conclusions are consistent with those in the references. In addition, the angles of twist and tension measurement tests in natural icing environment were carried out at Xuefeng Mountain National Observatory of Energy Equipment Security of Chongqing University, and the results were compared with those obtained from the simplified model to further verify the feasibility of the proposed simplified model.

## II. METHODOLOGY

### A. New Simplified Model for Torsion of Single Conductor with Light Icing

The icing torsion process of a single conductor is a gradual development process. The ice first accumulates on the windward side, and when the ice accretion reaches a certain thickness, the conductor will twist to a certain extent under the action of eccentric torque and then maintains the torque balance state. Then ice accretion continues to grow on the new windward side, repeating the process of ‘eccentric icing growth-torsion-balance’ until the icing ends.

Combined with the aforementioned physical process of natural icing, and taking into account the convenience of computer operations, this paper constructs a new model for torsion of ice-coated single conductor based on the following simplified calculation assumptions:

① Assuming that the ice shape is a typical crescent shape, the annular ice with a given thickness  $h$  is equivalent to the corresponding eccentric ice according to the principle of area equivalence (shown in Fig. 2). Considering the difference in ice thickness between the windward side and the leeward side, the traditional assumption that the semi-ellipse is approximately a whole crescent shape is abandoned [10], and only the ice shape on the windward side is simplified to a standard semi-ellipse with the semimajor axis of  $a$ , while that on the leeward side is simplified to a standard semicircle with the radius of  $b$  (except for the initial ice shape);

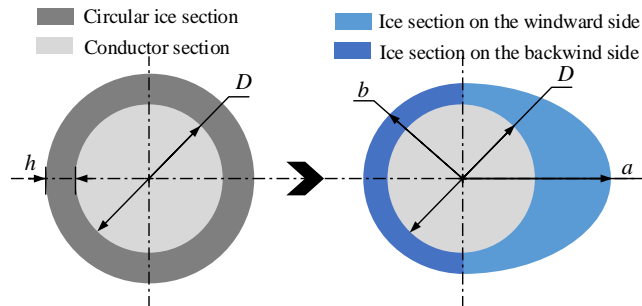


Fig. 2 Schematic diagram of the principle of area equivalence

② The new ice-covered layer will wrap around the old one and the overall ice shape remains a crescent shape in the horizontal direction, which is regarded as one of the geometric criteria for updating ice weight and torque (shown in Fig. 3);

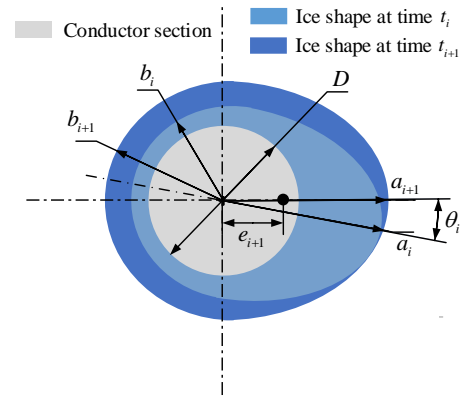


Fig. 3 Schematic diagram of the updated ice shape

③ The influence of torsion caused by existing ice on the torsional stiffness of conductors is considered in the model while the influence of existing ice itself on the torsional stiffness of conductor is ignored;

④ The angles of twist after each icing conform to the principle of small deformation to ensure the rationality of the applied icing torque;

⑤ For the initial icing, consider the uniform icing within the whole span and then update the ice weight and ice torque according to the differences in angles of twist at different positions.

Based on the above assumptions, the update formulas of the equivalent ice torque acting on the unit length conductor at  $t_{i+1}$  can be expressed as:

$$T_{i+1} = A_{i+1} \rho g e_{i+1} = \frac{2\rho g b_{i+1} (2a_{i+1} b_{i+1} + 2b_{i+1}^2 - D^2) (a_{i+1}^2 - b_{i+1}^2)}{2a_{i+1} b_{i+1} + 2b_{i+1}^2 - D^2} \quad (1)$$

$$a_{i+1} = a_i + \Delta a_{i+1} \quad (2)$$

$$b_{i+1} = a_{i+1} a_i \frac{|\sin \theta_i|}{\sqrt{a_{i+1}^2 - a_i^2 \cos^2 \theta_i}} \quad (3)$$

Where  $T_{i+1}$ ,  $A_{i+1}$ ,  $e_{i+1}$ ,  $a_{i+1}$ ,  $b_{i+1}$ , and  $\Delta a_{i+1}$  are torque, ice cross-sectional area, the distance between ice cross-sectional centroid and conductor cross-sectional centroid, the semimajor axis of semi-elliptical ice on the windward side, the radius of circular ice on the leeward side and the increased ice thickness on the windward side at  $t_{i+1}$ ;  $\theta_i$  is the angle of twist caused by the torque at  $t_i$ ;  $\rho$  is the ice density;  $g$  is gravity acceleration and  $D$  is the diameter of the conductor.

### B. Algorithm Implementation of Model

In this paper, the algorithm of the torsion model is realized by using the Mechanical APDL (a sub-module of the commercial software ANSYS), and specifically:

① The structure parameters of overhead single conductors (shown in Table I) are set based on the prototype of a 110 kV transmission line project in Chongqing, China;

② For tension settings, based on the original design safety factor of 3.1, 2 groups of safety factors of 2.5 and 2 are added in this paper, i.e., 3 groups of pay-off tensions are set, which are 36.01 kN, 44.65 kN, and 55.81 kN;

③ In the selection of equivalent annular ice thickness, considering that the linear range of torsional stiffness of the

actual single conductor is limited, and when the actual torsional angle is too large, it may exceed the elastic deformation range of the conductor, and even plastic deformation or yield occurs, which is out of the scope of application of the aforementioned simplified model. Therefore, the value of the equivalent ice thickness should not be too large, and 3 groups of 2.5mm, 5mm, and 7.5mm are selected here;

④ In terms of software, the suspension points at the two ends are fully constrained by the degree of freedom of displacement, and considering the rotation effect of the insulator strings and suspension points, as well as the deformation of the conductor itself, only the torsional degree of freedom in the axial direction of the conductor at the two ends is constrained. The classical form-finding method of suspension cable is used to solve the initial geometric shape of the single conductor before icing.

TABLE I. STRUCTURAL PARAMETERS OF 110 kV TRANSMISSION LINE

Structural Parameters(Unit)	Values
Horizontal Span- $L$ (m)	230
Elevation Difference- $H$ (m)	0
Cross-sectional Area- $A$ (mm <sup>2</sup> )	297.57
Linear Mass- $\omega$ (kg/m)	1.0705
Rated Tensile Strength-RTS(N)	117501
Safety Factor- $K$	3.1
Tension- $T_0 = 0.95RTS / K (\times 10^4\text{N})$	3.6008
Modulus of elasticity- $E$ (Mpa)	77000

The algorithm implementation process based on the APDL command stream is shown in Fig. 4.

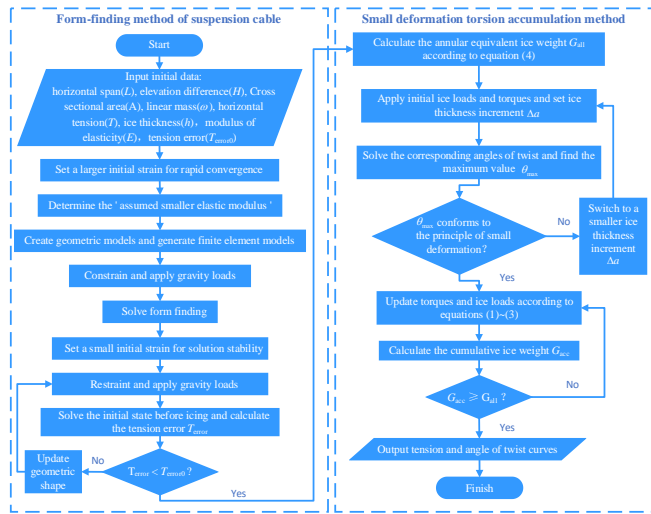


Fig. 4 Flow chart of the whole algorithm

$$G_{all} = \pi \rho g h (D + h) L \quad (4)$$

Where  $G_{all}$  is the annular equivalent ice weight and  $L$  is the length of the horizontal span.

### C. Effect of Pay-off Tensions on Torsion Process

In this paper, the angles of twist of the single conductor under 3 groups of pay-off tensions and 3 groups of ice thicknesses are calculated and the distribution curves within the span after icing are plotted in Fig. 5~7.

It can be seen from Fig. 5 ~7 that:

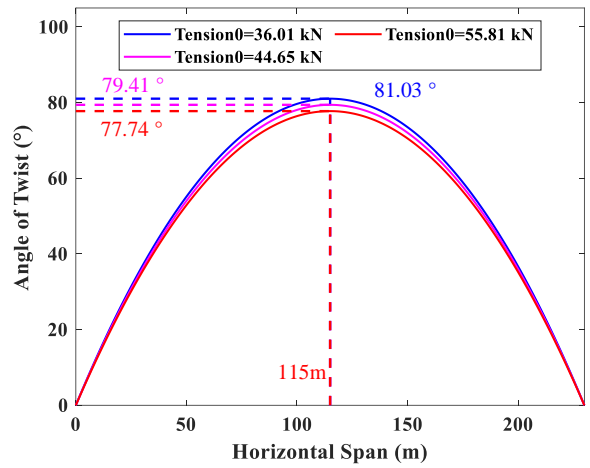


Fig. 5 Angle of twist distribution curves of 2.5mm icing under 3 groups of pay-off tensions

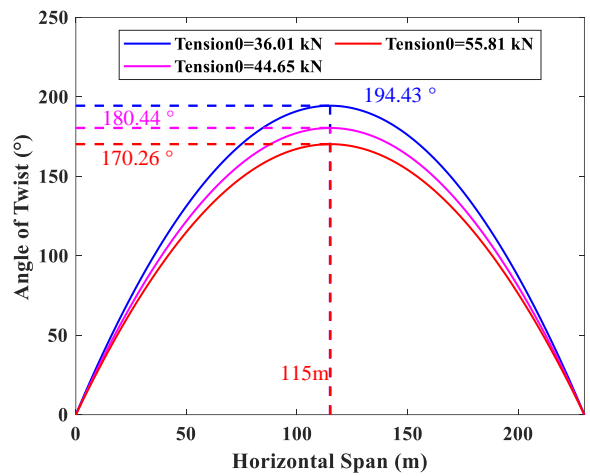


Fig. 6 Angle of twist distribution curves of 5mm icing under 3 groups of pay-off tensions

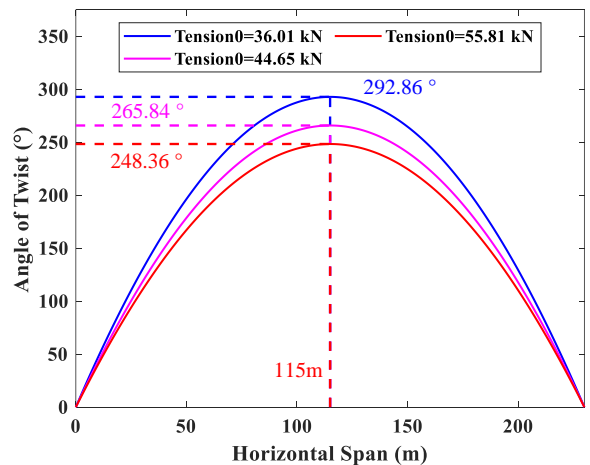


Fig. 7 Angle of twist distribution curves of 7.5mm icing under 3 groups of pay-off tensions

① Since there is no elevation difference between the two suspension points and the initial icing is considered to be uniformly distributed in the span, the final torsion results are all distributed symmetrically about the midpoint of the span(115m) where angles of twist reach the maximum value;

② Under the given three sets of tensions, regardless of the icing conditions, the suppression effect on torsion increases with the increase of tensions. Therefore, in order to suppress the torsion process as much as possible to reduce the ice accretion, the tension values should be set to the maximum allowable value of the project.

③ The calculation results of the given three sets of ice thicknesses showed that compared with the cumulative angles of twist of the whole span under the operating tension ( $K=3.1$ ,  $T_0=36.01$  kN), the other two groups of tensions are reduced by [2.01%, 4.06%] (2.5mm icing), [7.20%, 12.43%] (5mm icing) and [9.13%, 15.02%] (7.5mm icing). It can be seen that when the equivalent ice thickness is small, the increase of tensions has little effect on the torsion suppression effect, but the effect becomes more obvious with the increase of equivalent ice thickness.

To further explore the causes of such phenomena, /debug (a command in APDL) is used to obtain the torsional stiffness in the element stiffness matrix of the intermediate element of the span. The torsional stiffness curves and the tension curves of the corresponding element during the icing period are plotted in Fig. 8~10.

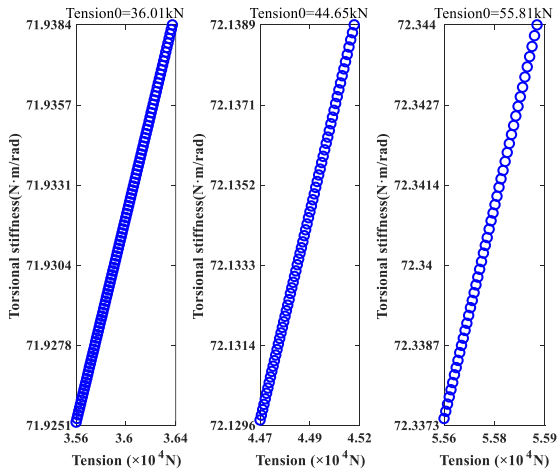


Fig. 8 Curves of torsional stiffness of intermediate element of the span under 2.5mm icing

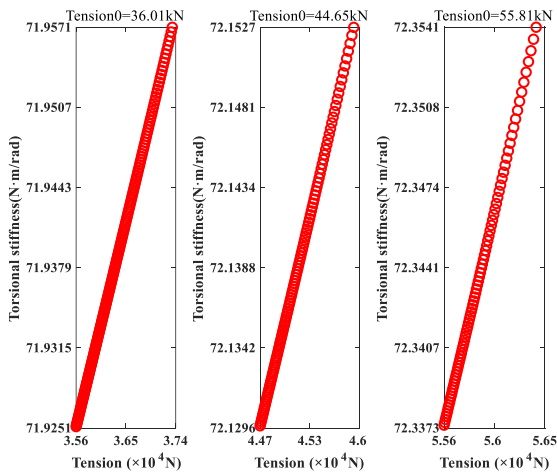


Fig. 9 Curves of torsional stiffness of intermediate element of the span under 5mm icing

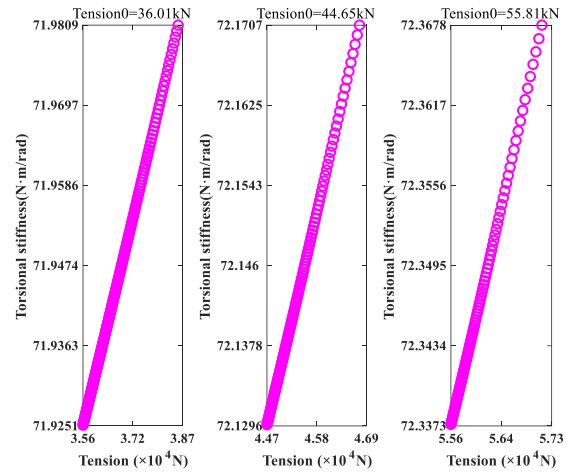


Fig. 10 Curves of torsional stiffness of intermediate element of the span versus tension under 7.5mm icing

It can be seen from Fig. 8 ~10 that:

① Before icing, the starting points of the torsional stiffness under different pay-off tensions are different, so increasing the tensions can increase the torsional stiffness of the intermediate element of the span, but the increment is not large (related to the type of constraints at its both ends);

② With the progress of the icing process, the tension of the intermediate element increases continuously, but the corresponding increase in torsional stiffness is slightly smaller (less than 0.1%). Therefore, in the rough calculation, it can be approximately considered that the torsional stiffness of the conductor element near the middle of the span remains unchanged (ignoring the effect of the ice layer on torsional stiffness), which is consistent with the conclusion in [6].

#### D. Field Tests

The field tests were carried out at Xuefeng Mountain National Observatory of Energy Equipment Security of Chongqing University and the layout of the field test platform is shown in Fig. 11.

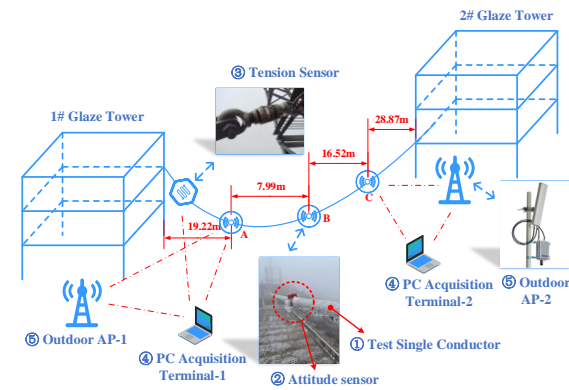


Fig. 11 Schematic diagram of field tests

Where ① is the test single conductor whose specific type is LGJ 400/35, and its detailed parameters are shown in Table II. ② is the attitude sensor, which is mainly used to obtain the angle of twist at the specified position. Its dynamic and static accuracy is  $0.1^\circ$  and  $0.05^\circ$ , respectively, and the sampling

rate is adjustable within the range of 20~200 Hz. In this test, a total of 3 attitude sensors (labeled A, B, and C) were arranged with their relative positions shown in the red dimensioning in Fig. 11, and the sampling rate was uniformly set to 50 Hz; The tension sensor ③ is installed at the suspension point to obtain the real-time tensions during the icing period, and its dynamic accuracy is 1 N. ④ is the PC acquisition terminals for real-time monitoring and storage of field test data. ⑤ is the outdoor AP machines, which are used to realize the LAN coverage of the test base, so as to transmit data wirelessly between the attitude sensors and the PC acquisition terminals.

TABLE II. STRUCTURAL PARAMETERS OF FIELD TEST LINE

Structural Parameters	Values
Horizontal Span- $L$ (m)	72.60
Elevation Difference- $H$ (m)	5.75
Cross-sectional Area- $A$ (mm <sup>2</sup> )	425.24
Linear Mass- $\omega$ (kg/m)	1.349
Modulus of elasticity- $E$ (Mpa)	65000

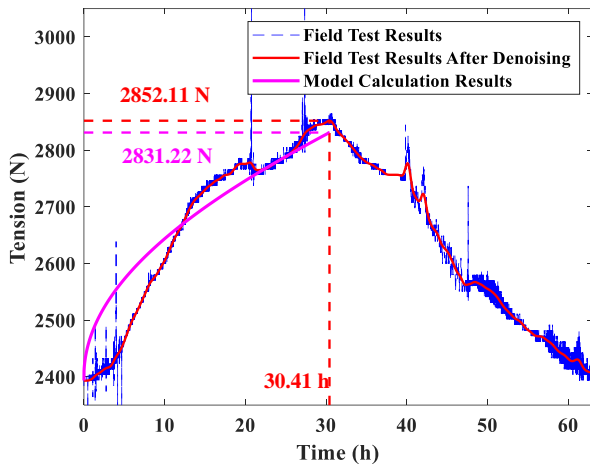


Fig. 12 Time-history curves of tension at the suspension point

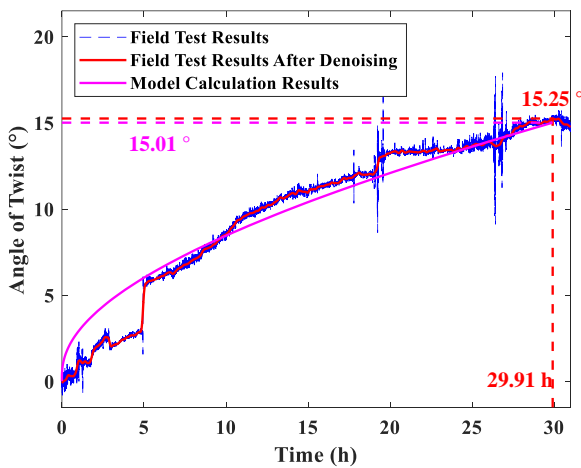


Fig. 13 Time-history curves of angles of twist of attitude sensor-A

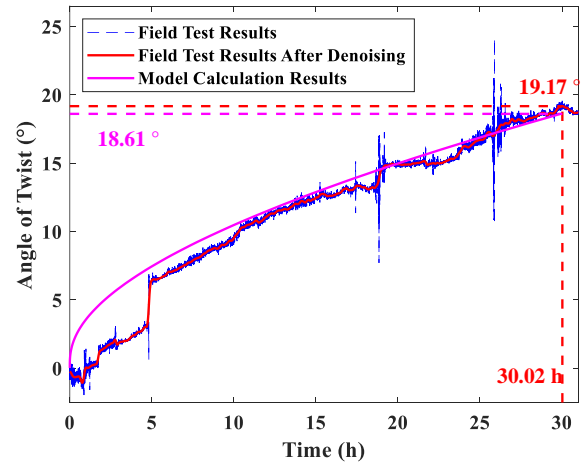


Fig. 14 Time-history curves of angles of twist of attitude sensor-B

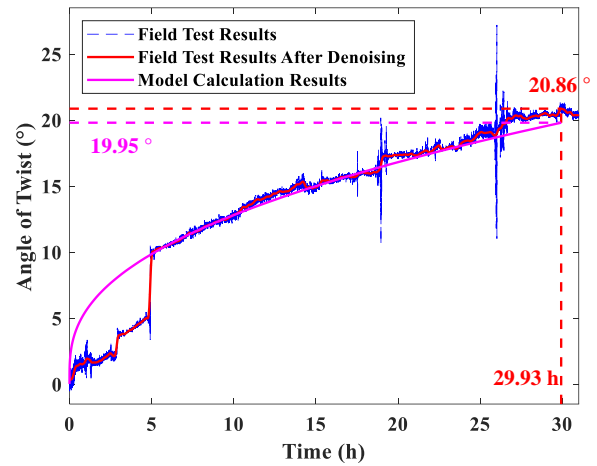


Fig. 15 Time-history curves of angles of twist of attitude sensor-C

The icing data of the field test are brought into the aforementioned simplified model of torsion, and the corresponding time-history curves of angles of twist and tensions are calculated, which are plotted together with the field measurement results in Fig. 12 ~ 15:

① The peak time of each curve is concentrated around 30h after the icing started, indicating that the ice has been growing eccentrically, resulting in the increase of angles of twist for most of the time;

② The error calculation results after icing completion show that the relative errors of the tensions and the angles of twist of the three positions (A - B - C) compared with the measured values are 0.73 %, 1.57 %, 2.92 %, and 4.36 %, respectively, which are less than 5 %, so the torsion calculation model shows good applicability in this icing;

③ Due to the limitation of the site location, the ice thickness and ice density data at the middle of the span cannot be obtained. Therefore, the ice equivalent parameters of the whole span obtained by encrypting the sampling points at other positions and taking the mean value will be smaller than the real values, which results in the smaller simulation results than the measured, whether the tensions at the suspension point or the angles of twist.

### III. CONCLUSIONS

(1) Ignoring the influence of the ice layer on torsional stiffness, it can be considered that the torsional stiffness of the conductor elements near the middle of the span remains constant during light icing;

(2) Under the light icing condition, the effect of tension increase on the torsion suppression is not obvious, but it shows that the effect of tensions becomes more and more obvious with the increase of equivalent ice thickness;

(3) The simplified calculation model of torsion of single conductors proposed in this paper has good applicability within the elastic deformation range of the conductor (under light icing conditions), but further research is still needed to extend it to medium and heavy icing conditions.

### ACKNOWLEDGMENT

This work was supported by graduate research and innovation foundation of Chongqing, China (CYB20016 and CYB21019).

### REFERENCES

- [1] M. Farzaneh, *Atmospheric Icing of Power Networks*, 2nd ed., Springer Netherlands, 2008.
- [2] M. Farzaneh, "Ice accretions on high-voltage conductors and insulators and related phenomena," *A Math. Phys. Eng.*, vol. 358, pp. 2971–3005, Nov. 2000.
- [3] X.L. Jiang, L.C. Shu, "Chinese transmission lines icing characteristics and analysis of severe ice accidents," *Int. J. Offshore Polar Eng.*, vol. 14, pp. 196–201, Sept. 2004.
- [4] P. Li, J. Fan, W. Li, Z. Su, and J. Zhou, "Flashover performance of HVDC iced insulator strings," *IEEE Trans. Dielectr. Electr. Insul.* vol. 14, pp. 1334–1338, May 2007.
- [5] Y. Chen, M. Farzaneh, E.P. Lozowski, and K. Szilder, "Modeling of ice accretion on transmission line conductors," In IWAI 2000, Proceedings of the 9th International Workshop on Atmospheric Icing of Structures, Chester, UK, 5-8 June 2000. EA Technology Limited, Capenhurst, UK. Session 4b.
- [6] P. Fu, M. Farzaneh, "Simulation of the ice accretion process on a transmission line cable with differential twisting," *CANADIAN JOURNAL OF CIVIL ENGINEERING*, vol. 34, pp. 147-155, Feb. 2007.
- [7] R. Keutgen, J.L. Lilien and T. Yukino, "Transmission line torsional stiffness. Confrontation of field-tests line and finite element simulations," *IEEE Trans. Power Del.*, vol. 14, no. 2, pp. 567-578, Apr. 1999.
- [8] S.X. Fan, G.J. He, and X.P. Liao, "Experiment on torsional stiffness of ice-coated conductor," (in Chinese) *ELECTRICAL POWER*, vol. 38, pp.10, Mar. 2005, doi: 10.3969/j.issn.1004-9649.2005.10.010.
- [9] O. Nigol, P. G. Buchan, "Conductor Galloping-Part II Torsional Mechanism," *IEEE Transactions on Power Apparatus & Systems*, vol. 100, no. 2, pp. 708-720, Nov. 1981.
- [10] B.H. Lu, J. Liu, Z.J. Zhang, Y. Lei, H.T. Fu, "Research on an Optimal Design Method of Anti-Icing and Anti-Galloping Device Based on Loading Principle," *ICEMPE 2021 -3rd International Conference on Electrical Materials and Power Equipment*, April 11, 2021.